Elsevier Editorial System(tm) for Journal of Sound and Vibration
Manuscript Draft

Manuscript Number:

Title: Simulation and experimental validation of the dynamical model of a dual-rotor vibrotactor

Article Type: SI: ICOVP-2013

Section/Category: A Active and adaptive control of sound and vibration

Keywords: dual-rotor vibrotactor; self-synchronization; haptics; vibroactuator; tactile feedback

Corresponding Author: Mr. Akos Miklos,

Corresponding Author's Institution: HAS-BUTE

First Author: Akos Miklos

Order of Authors: Akos Miklos; Zsolt Szabo, PhD

Abstract: In this work, a novel design for small vibrotactors called Dual Excenter is presented, which makes it possible to produce vibrations with independently adjustable frequency and amplitude. This feature has been realized using two coaxially aligned eccentric rotors, which are driven by DC motors independently. The prototype of the device has been built, where mechanical components are integrated on a frame with two optical sensors for the measurement of angular velocity and phase angle. The system is equipped with a digital controller. Simulations confirm the results of analytical investigations, and they allow us to model the sampling method of the signals of the angular velocity and the phase angle between the rotors. Furthermore, we model the discrete behaviour of the controller, which is a PI controller for the angular velocities, and a PID controller for the phase angle. Finally, simulation results are compared to experimental ones, which show that the Dual Excenter concept is feasible.

Simulation and experimental validation of the dynamical model of a dual-rotor vibrotactor

Á. Miklós[a,b,*], Z. Szabó[b]

[a] *Research Group on Dynamics of Machines and Vehicles, HAS-BUTE, Műegyetem rkp. 5, 1111 Budapest, Hungary*
[b] *Department of Applied Mechanics, Budapest University of Technology and Economics, Műegyetem rkp. 5, 1111 Budapest, Hungary*

Abstract

In this work, a novel design for small vibrotactors called Dual Excenter is presented, which makes it possible to produce vibrations with independently adjustable frequency and amplitude. This feature has been realized using two coaxially aligned eccentric rotors, which are driven by DC motors independently. The prototype of the device has been built, where mechanical components are integrated on a frame with two optical sensors for the measurement of angular velocity and phase angle. The system is equipped with a digital controller. Simulations confirm the results of analytical investigations, and they allow us to model the sampling method of the signals of the angular velocity and the phase angle between the rotors. Furthermore, we model the discrete behaviour of the controller, which is a PI controller for the angular velocities, and a PID controller for the phase angle. Finally, simulation results are compared to experimental ones, which show that the Dual Excenter concept is feasible.

Keywords: dual-rotor vibrotactor, self-synchronization, haptics, vibroactuator, tactile feedback

1. Introduction

Transmitting information by mechanical vibrations has become an essential way in many personal, industrial and military applications [1]. Nowa-

*Tel.: +36 1 463 1436; fax: +36 1 463 3471
Email addresses: miklosa@mm.bme.hu (Á. Miklós), szazs@mm.bme.hu (Z. Szabó)

days cell phones could hardly be imagined without the vibration alert, which makes it possible to inform the user about various events silently. The success of this feature inspired designers of many other personal or industrial handheld devices. As the visual perception of the man recognises only things which are in the direction of his sight, car manufacturers have developed applications to avoid hazardous events using sound or vibration signals [2, 3]. There are also vests and belts, which can aid the orientation of air force pilots by mechanical vibrations transmitted to the skin, indicating top or down directions, or direction of attack. This could not be done by visual or sound signals, because the visual and auditory processing capacity of the pilots may already be overloaded [4]. This way it is also possible to teach and guide different postures and movements by vibrotactile feedback to do physiotherapy for stroke patients [5].

Todays standard vibrotactors are DC motor driven eccentric rotors called eccentric rotating mass (ERM) vibrotactors. This concept allows a very simple design, but as the frequency and the amplitude of the excited vibrations are not independent, the performance of such devices is limited. In most common applications for vibrotactors like cell phones or video game controllers, the excited vibration has to be adjusted to the sensitivity of the users skin, so frequencies much higher than the optimum cannot be used due to possible pain caused by large amplitudes; while at frequencies lower than the optimum, the amplitude may go below the sensation threshold of the skin [6]. This way the standard ERM vibrotactor only enables the indication of an event. If the complexity of the transmitted information has to be increased, different vibration patterns could be used. The disadvantage of such solution is that the user has to interpret the meaning of the patterns, which puts additional cognitive load on him. However, the capability of mechanoreceptors in human skin to differentiate between different vibration parameters [7] could be used in a more intuitive way. Thus it is possible to transmit information by changing vibration amplitude and frequency separately. Also, in experimental applications where exact vibration parameters (amplitudes and frequencies) have to be set during operation, simple vibrotactors like the ERM vibrotactors cannot be used.

The dual-rotor vibrotactor concept presented in this work — also called as Dual Excenter — solves the problem of the coupling of the vibration frequency and the amplitude. In this concept two coaxially positioned eccentric rotors are used for generating mechanical vibration. As the resulting vibration is the superposition of the vibrations of the two rotors, the amplitude

can be changed by the phase difference between them. With another words at a given angular speed of the rotors the resulting eccentricity of the whole system can be adjusted by tuning the position of the rotors relative to each other. This relative position can be identified as an angle between the rotors, named *phase angle*, and so it will be related to the amplitude of the excited vibration. Furthermore, the angular speed of the two rotors are related to the frequency of the excited vibration. Of course, the angular speed also limits the maximal available amplitude, since it is the linear function of the eccentricities (defined as mass times length) of the rotors and the quadratic function of the frequencies.

This way, a complex sensation can be generated on the human skin, or the excitation for a laboratory experiment can be set by selecting the amplitude and the frequency independently. The method is showed in Fig. 1 where different configurations are depicted. The small black circles show the centres of mass (CoM) of the rotors and the large circle represents the common CoM of the two rotors, respectively. If the angular speeds of both rotors are the same, the common CoM moves on a circular path as well. As it can be seen, the distance between the common CoM and the axis of rotation can be changed by the relative position of the CoMs of the rotors. Zero amplitude is only possible, if the eccentricities for both rotors are the same.

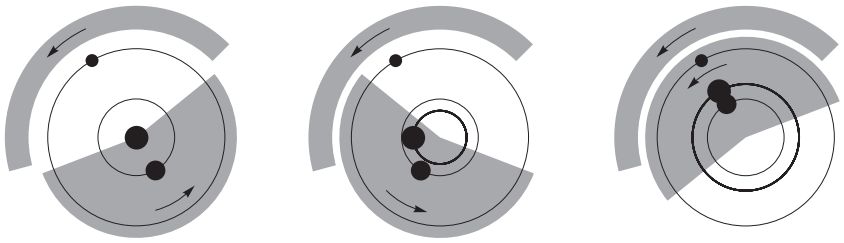

Figure 1: Different configurations of the rotors for (a) zero, (b) medium and (c) maximum amplitude.

The Dual Excenter concept solves not only the problem of the constrained coupling between frequency and amplitude, but it also enables some attractive working modes showed in Fig. 2. If the two rotors run in the same direction with different angular velocities, the resulting vibration will be a pulsating one. In case of opposite rotor directions and with equal angular velocities the vibration is one-directional rather than rotating, and with dif-

ferent angular speeds this direction can also be modified. In these latter cases the independent amplitude and frequency cannot be achieved.

The concept also enables fast changes in vibration amplitudes without slowing down and speeding up again the rotors, because only a change in the phase angle is needed. This can be carried out quickly and energy-efficiently.

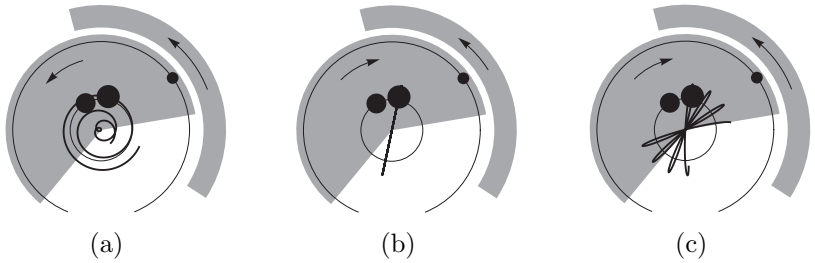

Figure 2: Further possible working modes of the Dual Excenter: (a) pulsating, (b) one-directional and (c) direction changing vibration.

2. Mechanical model of the dual-rotor vibrotactor

To investigate the feasibility of the novel Dual Excenter concept, a mechanical model has to be constructed. Doing this, the main components of such device have to be considered, which have significant influence on the dynamics of the system. One of the possible designs of the device is depicted in Fig. 3.

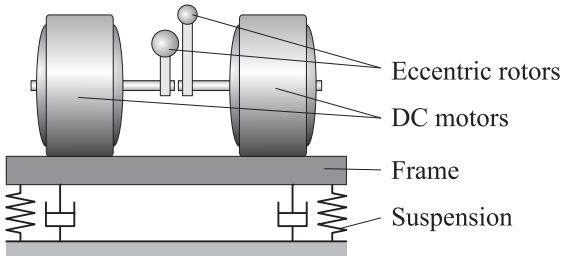

Figure 3: Main components of the Dual Excenter.

The main parts of the device are the two eccentric rotors, the driving DC motors, which are mounted on the frame. This frame can be suspended on any object (like the human skin or the frame of a cell phone). In simple case the suspension can be considered as a linear system of springs and dampers.

Generally, the motion of the frame could be 6 degrees-of-freedom spatial motion, however for analytical investigations some simplifications could be introduced. If the suspension of the system is considered as isotropic and the two CoMs of the eccentric rotors are rotating in the same plane (or approximately the same plane), the motion of the frame can be considered as planar motion. The plane of the motion is then normal to the common rotational axis [8]. Furthermore, both rotors and driving motors have the same physical parameters. Later experiments show that these simplifications do not limit the validity of the proposed mechanical model. The planar mechanical model of the device can be seen in Fig. 4.

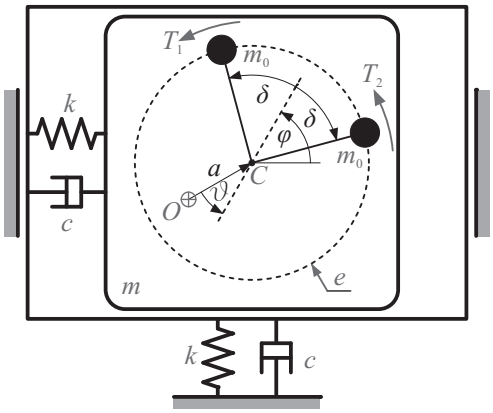

Figure 4: Planar mechanical model of the Dual Excenter.

In Fig. 4 point O is the origin of the global reference frame, which in case of undeformed springs coincides with point C, which represents the common rotational axis of the rotors. The position of point C is given by the polar coordinates a and ϑ. Furthermore, the angular positions of the two rotors are given by the anglular position of the common bisector of the rotors φ measured from the horizontal (this in turn indicates the angular position of the common CoM), and the angle between the rotors and the common bisector δ, which is actually the half of the phase angle of the rotors. So the mechanical model has 4 degrees-of-freedom. The suspension of the frame is parameterized by the spring stiffness k and damping coefficient c. The mass of the common frame is m, while m_0 and e are the mass and eccentricity (length) of both rotors, respectively. The mass moments of inertia of the rotors about the axis of rotation can be considered by the parameter J. The driving motors are taken into account by the torques T_1 and T_2, where the

stationary performance of the DC motors has been used as follows.

$$T = k_t \frac{u - k_e \omega}{R}, \tag{1}$$

where T is the stationary torque of the motor, k_t and k_e are the torque- and speed constant, u is the driving voltage, and R is the electric resistance of the motor coil.

The derivation of the dimensionless equations of motion in Eq. (2) can be found in [8], where c_Δ, c_Θ, s_Δ and s_Θ are the sine and cosine of angle Δ and Θ, respectively.

$$\begin{pmatrix} 1 & 0 & -\mathrm{c}_\Delta \mathrm{s}_\Theta & -\mathrm{s}_\Delta \mathrm{c}_\Theta \\ 0 & A & -A - \mathrm{c}_\Delta \mathrm{c}_\Theta & \mathrm{s}_\Delta \mathrm{s}_\Theta \\ -\mathrm{c}_\Delta \mathrm{s}_\Theta & -A^2 - A\,\mathrm{c}_\Delta \mathrm{c}_\Theta & 1 + A + 2A\,\mathrm{c}_\Delta \mathrm{c}_\Theta + k_1 & -A\,\mathrm{s}_\Delta \mathrm{s}_\Theta \\ -\mathrm{s}_\Delta \mathrm{c}_\Theta & A\,\mathrm{s}_\Delta \mathrm{s}_\Theta & -A\,\mathrm{s}_\Delta \mathrm{s}_\Theta & k_1 \end{pmatrix} \begin{pmatrix} A'' \\ \Theta'' \\ \Phi'' \\ \Delta'' \end{pmatrix}$$
$$= \begin{pmatrix} A\,(\Phi' - \Theta')^2 - 2\zeta A' - A + (\Phi'^2 + \Delta'^2)\,\mathrm{c}_\Delta \mathrm{c}_\Theta - 2\Phi'\Delta' \mathrm{s}_\Delta \mathrm{s}_\Theta \\ (2\zeta A + 2A')\,(\Phi' - \Theta') - (\Phi'^2 + \Delta'^2)\,\mathrm{c}_\Delta \mathrm{s}_\Theta - 2\Phi'\Delta' \mathrm{s}_\Delta \mathrm{c}_\Theta \\ 2\,(\zeta A^2 + A\,A' + A' \mathrm{c}_\Delta \mathrm{c}_\Theta)\,(\Theta' - \Phi') - A\,(\Theta'^2 - 2\Theta'\Phi' - \Delta'^2)\,\mathrm{c}_\Delta \mathrm{s}_\Theta \\ \qquad + 2A\,\Phi'\Delta' \mathrm{s}_\Delta \mathrm{c}_\Theta + \Sigma U - r\,\Phi' \\ 2A'\,(\Phi' - \Theta')\,\mathrm{s}_\Delta \mathrm{s}_\Theta - A\,(\Theta' - \Phi')^2\,\mathrm{s}_\Delta \mathrm{c}_\Theta + \Delta U - r\,\Delta' \end{pmatrix}, \tag{2}$$

where capital letters A, Θ, Φ and Δ are the dimensionless pairs of the generalized coordinates a, ϑ, φ and δ, respectively. ζ is the damping ratio of the suspended frame, k_1 contains the inertial-, while r the electric parameters of the system. ΣU and ΔU are the dimensionless sum and the difference between the driving voltages, respectively. Prime denotes derivation with respect to the dimensionless time $\tau = t\,\alpha$, where t is the time in seconds and α is the eigenfrequency of the suspended frame. Assuming that

$$A = A_0,\ \Theta = \Theta_0,\ \Delta = \Delta_0 \text{ and } \Phi' = \lambda_0, \tag{3}$$

so all coordinates, except for Φ are constant, and $\lambda = \Phi'$, which is the frequency ratio between the angular velocity $\dot{\varphi}$ and the eigenfrequency α of the suspended frame, is also constant, the steady state motion of the system can be investigated. Substituting Eqs. (3) in the equations of motion (2) the formulae for a, ϑ and the sum and the difference between the driving voltages of the motors can be given as the functions of the frequency ratio and the Δ_0 half of the phase angle.

$$A_0 = \frac{\lambda_0^2 \cos\Delta_0}{\sqrt{\left(1-\lambda_0^2\right)^2 + \left(2\zeta\lambda_0\right)^2}}, \quad \tan\Theta_0 = \frac{2\zeta\lambda_0}{1-\lambda_0^2}, \tag{4}$$

$$\Sigma U = \frac{2\zeta\lambda_0^5 \cos^2\Delta_0}{\left(1-\lambda_0^2\right)^2 + \left(2\zeta\lambda_0\right)^2} + r\lambda_0 \;\text{ and }\; \Delta U = \frac{\lambda_0^4\left(1-\lambda_0^2\right)\cos\Delta_0 \sin\Delta_0}{\left(1-\lambda_0^2\right)^2 + \left(2\zeta\lambda_0\right)^2}. \tag{5}$$

The formulae in Eqs. (4) are very similar to the amplitude and phase delay of an eccentric excited oscillator. Nevertheless Eqs. (5) mean, that for every λ_0 and Δ_0 the values of the motor driving voltages can be given where the system has steady state motion characterized by the frequency ratio and the phase angle. To be able to realize such steady state motions the investigated working point should be stable. After the linear stability analysis of the working points $(\lambda_0; \Delta_0)$ a characteristic stability chart can be seen in Fig. 5. Here we can see that the stationary motion is stable around $\Delta_0 = 0$ below the resonance frequency of the suspended frame, which is in-phase motion of the rotors, and around $\Delta_0 = \pi/2$ above the resonance frequency, which is anti-phase motion.

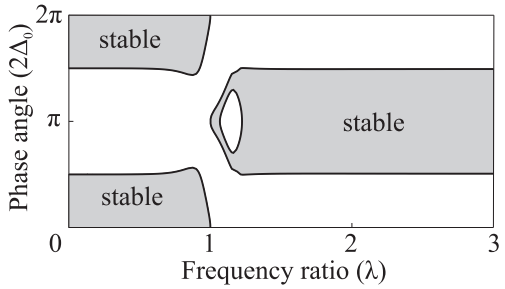

Figure 5: Characteristic linear stability chart for the Dual Excenter (with parameters listed in Table 1).

So even if the driving voltages are not equal, stationary motions can be observed in some regions, thus the rotors have the same angular speeds. This phenomenon is caused by the mechanical- or self-synchronization between the two eccentric rotors.

The mechanical synchronization was first investigated by Huygens, who experienced the synchronization of pendulum clocks attached to a common base [9]. Later many scientists worked on the theory of this phenomenon [10, 11, 12]. Recently Leonov showed a general method to handle with phase synchronization [13], and his work on the in-phase synchronization of two

metronome pendula shows, that there are still open problems in this area [14]. The work of Czolczynski et al. points out, that the mechanical synchronization occurs not only in unidirectional rotation of the eccentric rotors, but also with rotors turning in opposite direction [15]. Wen et al. investigated the planar motion vibratory screeners excited by two or four eccentric rotors [16, 17, 18].

In the following sections the mechanical synchronization of the system is investigated by means of simulations and experiments, and the possibility of stabilization of the whole working area of the Dual Excenter by a simple controller is analyzed.

3. Simulation results

For simulation purposes the chosen generalized coordinates showed in Fig. 4 are not convenient, because of the singularity of the polar coordinates around point O. For this reason instead of the polar coordinates of point C, translational coordinates x and y are introduced in simulations.

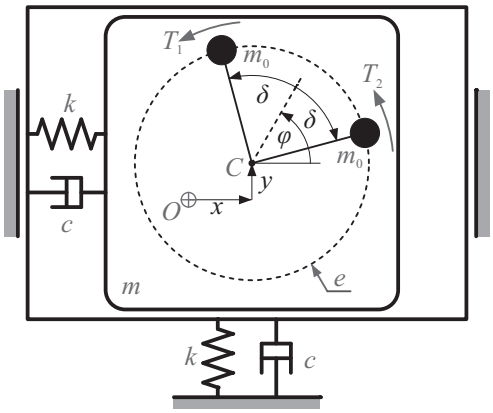

Figure 6: Mechanical model of the Dual Excenter with translational coordinates.

The modified equations of motion can be derived with the Lagrangian equation of the second kind. Introducing the parameter $E = e\,m_0$ the equations of motion have the form as Eq. (6).

$$\begin{pmatrix} m+2m_0 & 0 & -2E\cos\delta\sin\varphi & -2E\sin\delta\cos\varphi \\ 0 & m+2m_0 & 2E\cos\delta\cos\varphi & -2E\sin\delta\sin\varphi \\ -2E\cos\delta\sin\varphi & 2E\cos\delta\cos\varphi & 2J & 0 \\ -2E\sin\delta\cos\varphi & -2E\sin\delta\sin\varphi & 0 & 2J \end{pmatrix} \begin{pmatrix} \ddot{x} \\ \ddot{y} \\ \ddot{\varphi} \\ \ddot{\delta} \end{pmatrix}$$
$$= \begin{pmatrix} -k\,x - c\,\dot{x} + 2E\left(\dot{\delta}^2\cos\delta\cos\varphi - 2\dot{\delta}\dot{\varphi}\sin\delta\sin\varphi + \dot{\varphi}^2\cos\delta\cos\varphi\right) \\ -k\,y - c\,\dot{y} + 2E\left(\dot{\delta}^2\cos\delta\sin\varphi + 2\dot{\delta}\dot{\varphi}\sin\delta\cos\varphi + \dot{\varphi}^2\cos\delta\sin\varphi\right) \\ k_t\left(u_1 + u_2 - 2k_e\dot{\varphi}\right)/R \\ k_t\left(u_1 - u_2 - 2k_e\dot{\delta}\right)/R \end{pmatrix} \tag{6}$$

Based on the modified equations of motion numerical simulations have been carried out with the system parameters listed in Table 1, which are obtained from the experimental prototype device of the Dual Excenter in Fig. 7. The inputs for the simulation are the driving voltages of the two DC motors.

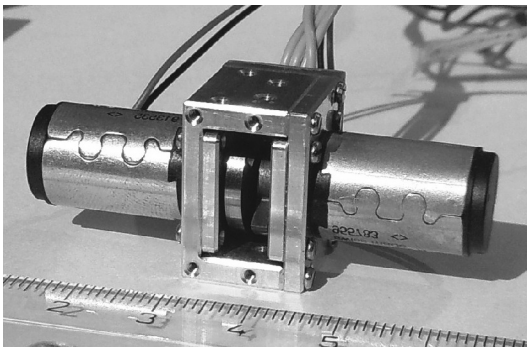

Figure 7: Prototype of the Dual Excenter.

First, the mechanical synchronization is investigated with different driving voltages, focusing on cases, where first the sum of the voltages changes, while the difference between them is held zero. The results of this simulation can be seen in Fig. 8. The initial phase angle between the two rotors is about 2 radians. Then, as the frequency increases, the mechanical synchronization brings the rotors in-phase. After reaching the resonance of the suspended frame, the phase angle quickly changes from zero to π.

Table 1: Parameters of the Dual Excenter prototype and simulation.

Name	Sign	Value	Unit
mass of the frame	m	42.1	g
eccentric mass of one rotor	m_0	1.6	g
inertia of one rotor	J	59.8	$\mathrm{g\,mm^2}$
eccentricity	e	2.1	mm
spring stiffness	k	5000	$\mathrm{N\,m^{-1}}$
damping coefficient	c	30	$\mathrm{N\,s\,m^{-1}}$
torque constant of one motor	k_t	5.08	$\mathrm{N\,mm\,A^{-1}}$
speed constant of one motor	k_e	5.08	$\mathrm{V\,s\,rad^{-1}}$
electric resistance of one motor	R	11.3	Ω

There is one more interesting effect: as the frequency approaches to the resonance, the amplitude of the vibration gets higher, which causes increased power consumption on the DC motors. This is called the jamming of electric motors [19]. So the passage through the resonance can only happen, if the driving voltage reaches a value large enough to cover this demand. This happens then with a characteristic jump in the frequency diagram.

In the second simulation the sum of the driving voltages is constant, and the difference between them is changed in steps. Fig. 9(a) shows the behaviour of the system above the resonance frequency, and Fig. 9(b) below the resonance. One can see that the frequencies of both rotors are the same as long as the voltage difference reaches a maximal value. Then the mechanical synchronization gets lost, and the rotors are turning with different angular velocities. As it could have been suspected, below the resonance with increasing voltage difference the system can be deviated from the in-phase (large amplitude) state, and the anti-phase domain is unstable. Above the resonance the behaviour is the opposite.

These results indicate that the system is capable to generate vibrations with different amplitudes at a given frequency, but the amplitude is limited to the stable regions, and it depends on the resonance frequency of the suspended frame as well. This makes the robust and optimal application of the device not possible.

For this reason a simple control is applied onto the system. Control of such system has been done by Liu et al., however the aim of their work

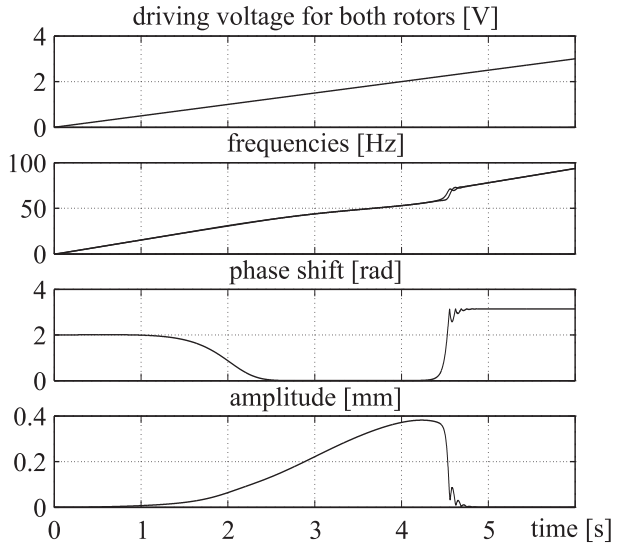

Figure 8: Stability of the system below and above the resonance frequency of the suspended frame.

was to achieve stable in-phase synchronization [17]. In this study only the feasibility of the control of the system is investigated, the control strategy and control parameters may not be the optimal ones.

The analytical investigations as well the simulations showed that the frequency of the generated vibration depends mainly on the sum of the driving voltages, and the phase angle at a given frequency can be adjusted by the voltage difference. These two inputs clearly define the driving voltages for the motors. The feedback for the control is the frequency and the phase angle, which can be measured e.g. by optical sensors on both rotors. In the current prototype the rotors are manufactured that way that the signal of the optical sensors changes in every turn twice. The frequencies f_1, f_2 and phase angle $\varepsilon = 2\delta$ can be calculated from the time required for every signal change and from the delay between the changes of the two sensors, respectively. Knowing these values the input voltages can be given by Eqs. (7) and (8).

$$\Sigma u_{\mathrm{ctrl}} = \Sigma u_{\mathrm{steady}} + P_{\mathrm{frq}} \left(f_{\mathrm{desired}} - \frac{f_1 + f_2}{2} \right) \tag{7}$$

$$\Delta u_{\mathrm{ctrl}} = \Delta u_{\mathrm{steady}} + P_{\mathrm{eps}} \left(\varepsilon_{\mathrm{desired}} - \varepsilon \right) + D_{\mathrm{eps}} \dot{\varepsilon} \tag{8}$$

where the steady voltage values can be calculated from Eqs. (5). The P and

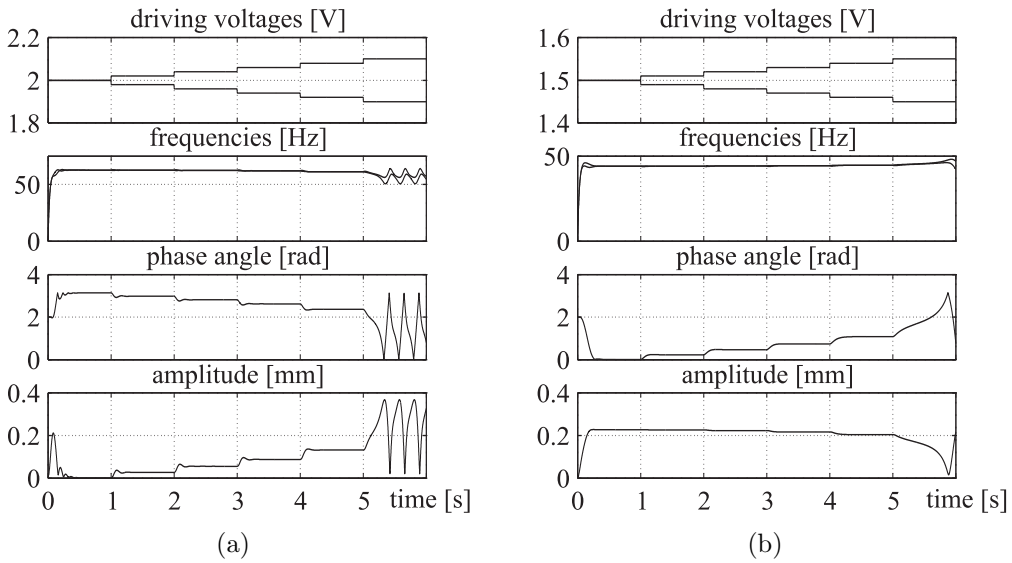

Figure 9: Influence of the voltage difference on phase angle (a) above and (b) below the resonance frequency.

D parameters are proportional and differential gains, respectively. The first derivative of the phase angle can be obtained from the difference between the angular velocities.

With this control strategy simulations were carried out, where the effects of a digital control were taken into account, like digital sampling, time delay of the sampling of frequency and phase angle, time delay of control signal, and discrete values of the control signals. The results of a simulation can be seen in Fig. 10. One can see that with control parameters optimized for a frequency around 80 Hz the control of the phase angle is possible with good performance. However, if the frequency decreases, the stability of the control loses because of the increased time delay in the signal feedback, and at higher frequencies the accuracy of the control deteriorates because of high forces, returning the system in stable regions.

4. Experimental results

The results obtained from simulation were validated by measurements on the prototype device showed in Fig. 7. First, the measurement according to the simulation in Fig. 9(a) was carried out, as it can be seen in Fig. 11. Since the suspension parameters of the measurement were practically unknown (the

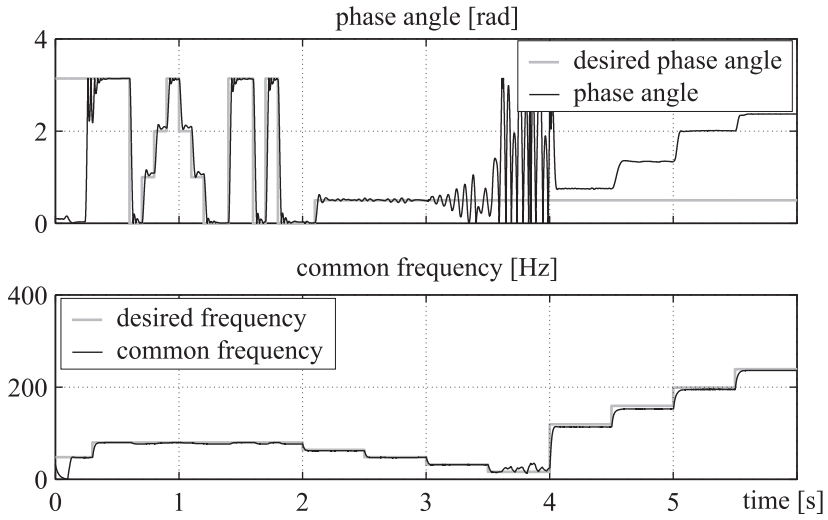

Figure 10: Performance of the controlled system for different angular velocity domains.

device has been held by hand), the measurement and the simulation show very good match, so the possibility of the uncontrolled application has been verified, however the performance of such a device would be very poor since the stable phase angle range is limited.

As it can be clearly seen, the control is needed for the optimal and robust application of the device. For the prototype device a very similar control has been implemented as in Eqs. (7) and (8) with the difference that instead of the steady voltage values an integral term has been used in both voltage sum and difference expressions because of the uncertain system parameters.

Fig. 12 shows the performance of the realized control. One can see that the accuracy of the control is not as good as in the simulation, and in the unstable domain some disturbances occur (at time = 80 s). The reasons for these effects are: first the control parameters are not optimal, so the control could be further developed; second, the implementation of the digital control is still in development stage. There are some communication and implementation issues, which will be handled later, e.g. the integral term is reset at every update of the desired values, so there is a jump in the signal of the phase angle at every new demand. However, the measurements show clearly that the control is possible in stable and unstable domains as well, even with only two sampled signals per turn.

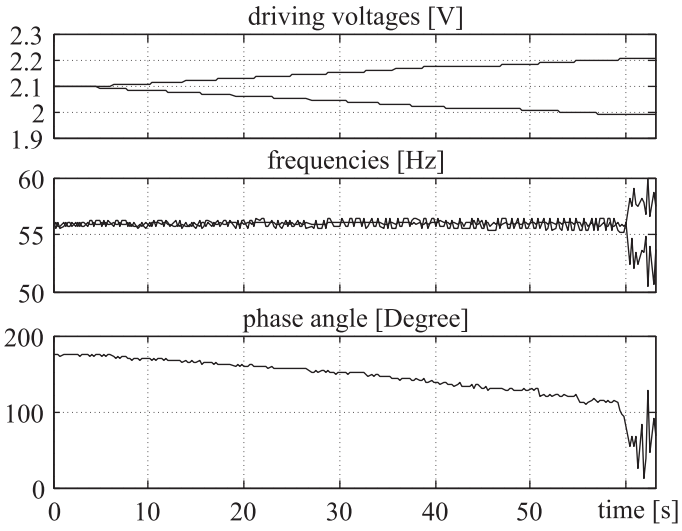

Figure 11: Measurement of the phase angle at different voltage differences above resonance.

5. Conclusions and outlook

In the present paper we showed a novel vibrotactor concept called Dual Excenter. With this dual-rotor design it is possible to generate vibrations with independent frequency and amplitude. This way one of the major limitations of simple ERM vibrotactors could be avoided.

After the Dual Excenter concept has been introduced, analytical investigations have been carried out to explore the dynamical behaviour of the dual-rotor system. For this reason a 4 degrees-of-freedom mechanical model was used with some idealization. Then stationary motions and their linear stability were investigated, and the effect of the self-synchronization has been revealed. This synchronization enables the use of the device without control, but this kind of operation limits the working area to the stable stationary motions.

To investigate the possibility of a controlled operation, simulations were performed, where the effects of the digital control have been taken into account as well. The simulations proved the results of the analytical investigations, and they allowed us to construct the prototype of the Dual Excenter. Measurements were carried out to test the prototype device in real environment, and the results were encouraging. Although neither the control strategy nor the control parameters were optimized, it was possible to set vibration frequency and amplitude to the desired value with good accuracy and

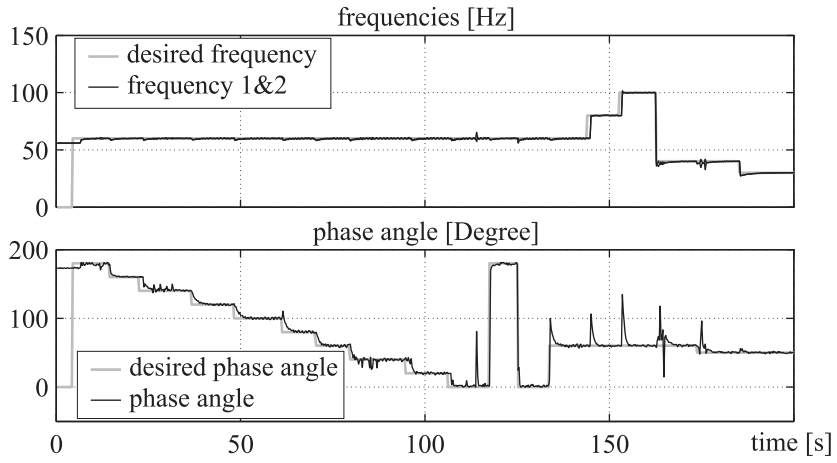

Figure 12: Performance of the PID controlled Dual Excenter.

short response time. The measurements showed also that the used mechanical model was a good approximation of the real device, and the idealizations which were introduced have not limited the usability of it.

The overall results of this paper showed, that the Dual Excenter device fulfils the aim of the independent frequency and amplitude, thus it is feasible to use it for generating advanced haptic feedback for applications listed in the Introduction.

Acknowledgement

This work was supported in part by the Hungarian National Development Agency under Intergovernmental S&T Cooperation Grant TÉT_08-SG-2010-0002, project name COSMOSYS.

References

[1] M. A. Srinivasan, C. Basdogan, Haptics in virtual environments: Taxonomy, research status, and challenges, Computers & Graphics 21 (4) (1997) 393 – 404. doi:10.1016/S0097-8493(97)00030-7.

[2] C. Ho, H. Z. Tan, C. Spence, Using spatial vibrotactile cues to direct visual attention in driving scenes, Transportation Research Part F: Traffic Psychology and Behaviour 8 (6) (2005) 397 – 412. doi:10.1016/j.trf.2005.05.002.

[3] C. Ho, H. Z. Tan, C. Spence, Multisensory in-car warning signals for collision avoidance, Human Factors: The Journal of the Human Factors and Ergonomics Society 49 (6) (2007) 1107 – 1114. doi:10.1518/001872007X249965.

[4] J. van Erp, B. Self, Tactile displays for orientation, navigation and communication in air, sea and land environments, Final report, NATO Science and Technology Organization (August 2008).

[5] Z. Q. Ding, Z. Q. Luo, A. Causo, I. M. Chen, K. X. Yue, S. H. Yeo, K. V. Ling, Inertia sensor-based guidance system for upperlimb posture correction, Medical Engineering & Physics 35 (2) (2013) 269 – 276. doi:10.1016/j.medengphy.2011.09.002.

[6] D. A. Mahns, N. M. Perkins, V. Sahai, L. Robinson, M. J. Rowe, Vibrotactile frequency discrimination in human hairy skin, J Neurophysiol 95 (3) (2006) 1442 – 1450. doi:10.1152/jn.00483.2005.

[7] A. J. Brisben, S. S. Hsiao, K. O. Johnson, Detection of vibration transmitted through an object grasped in the hand, Journal of Neurophysiology 81 (4) (1999) 1548–1558.

[8] A. Miklos, Z. Szabo, Vibrator with DC motor driven eccentric rotors, Periodica Polytechnica Mechanical Engineering 56 (1) (2012) 49 – 53. doi:10.3311/pp.me.2012-1.08.

[9] C. Huygens, Horologium Oscillatorium, Apud F. Muguet, Paris, France, 1673.

[10] I. Blekhman, A. Fradkov, H. Nijmeijer, A. Pogromsky, On self-synchronization and controlled synchronization, Systems & Control Letters 31 (5) (1997) 299 – 305. doi:10.1016/S0167-6911(97)00047-9.

[11] I. Blekhman, A. Fradkov, O. Tomchina, D. Bogdanov, Self-synchronization and controlled synchronization: general definition and example design, Mathematics and Computers in Simulation 58 (46) (2002) 367 – 384. doi:10.1016/S0378-4754(01)00378-0.

[12] H. Nijmeijer, A dynamical control view on synchronization, Physica D: Nonlinear Phenomena 154 (34) (2001) 219 – 228. doi:10.1016/S0167-2789(01)00251-2.

[13] G. A. Leonov, Phase synchronization: Theory and applications, Automation and Remote Control 67 (10) (2006) 1573 – 1609. doi:10.1134/S0005117906100031.

[14] N. Kuznetsov, G. Leonov, H. Nijmeijer, A. Pogromsky, Synchronization of two metronomes, IFAC Proceedings Volumes (IFAC-PapersOnline) 3 (1) (2007) 49 – 52. doi:10.3182/20070829-3-RU-4912.00007.

[15] K. Czolczynski, P. Perlikowski, A. Stefanski, T. Kapitaniak, Synchronization of pendula rotating in different directions, Communications in Nonlinear Science and Numerical Simulation 17 (9) (2012) 3658 – 3672. doi:10.1016/j.cnsns.2012.01.014.

[16] Q. K. Han, B. C. Wen, Stability and bifurcation of self-synchronization of a vibratory screener excited by two eccentric motors, Adv. Theor. Appl. Mech. 1 (3) (2008) 107 – 119.

[17] X. Liu, C. Wang, C. Zhao, B. Wen, Observation and control of phase difference for a vibratory machine of plane motion, in: 2010 International Conference on Computer, Mechatronics, Control and Electronic Engineering (CMCE 2010), Vol. 4, 2010, pp. 330 – 334. doi:10.1109/CMCE.2010.5610130.

[18] C. Y. Zhao, B. C. Wen, X. L. Zhang, Synchronization of the four identical unbalanced rotors in a vibrating system of plane motion, Science China Technological Sciences 53 (2) (2010) 405–422. doi:10.1007/s11431-009-0376-x.

[19] G. Leonov, The passage through resonance of synchronous electric motors mounted on an elastic base, Journal of Applied Mathematics and Mechanics 72 (6) (2008) 631 – 637. doi:10.1016/j.jappmathmech.2009.01.015.

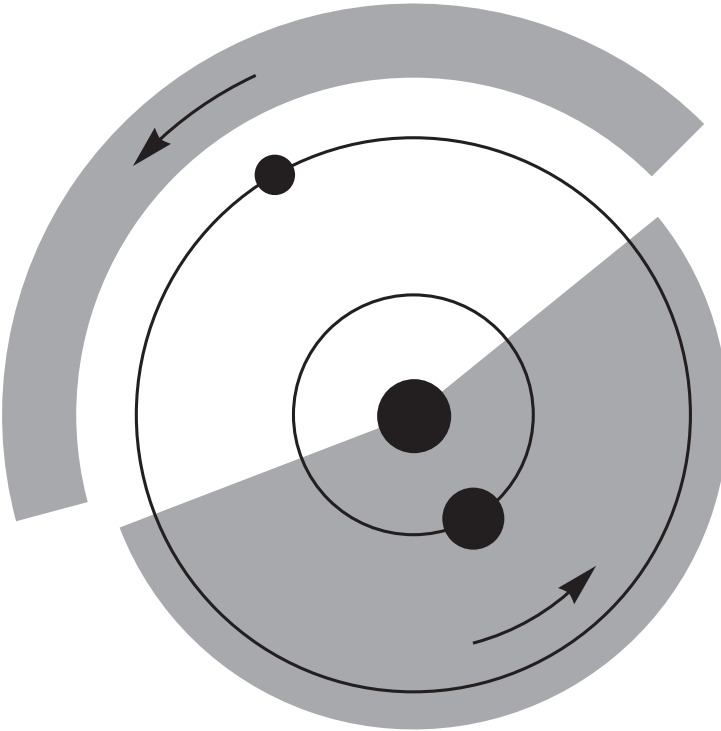

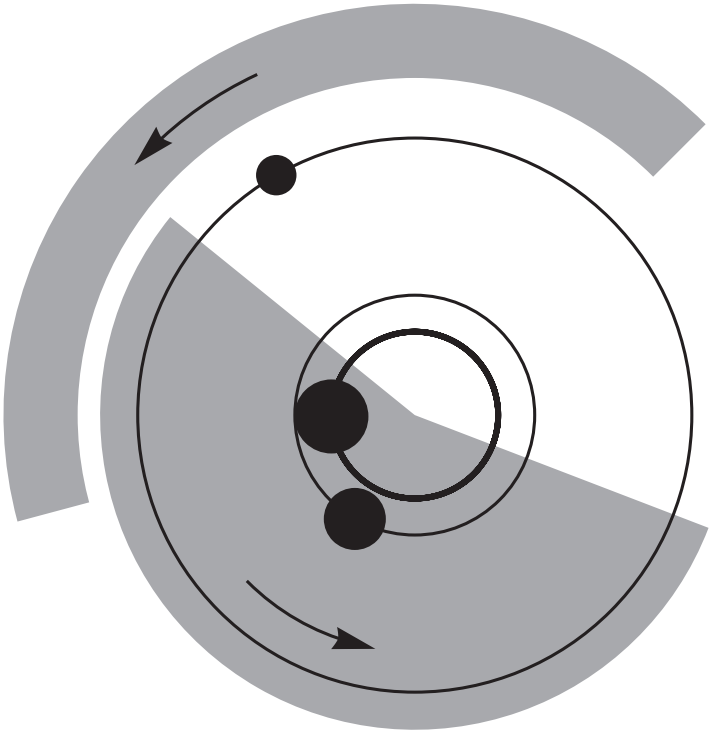

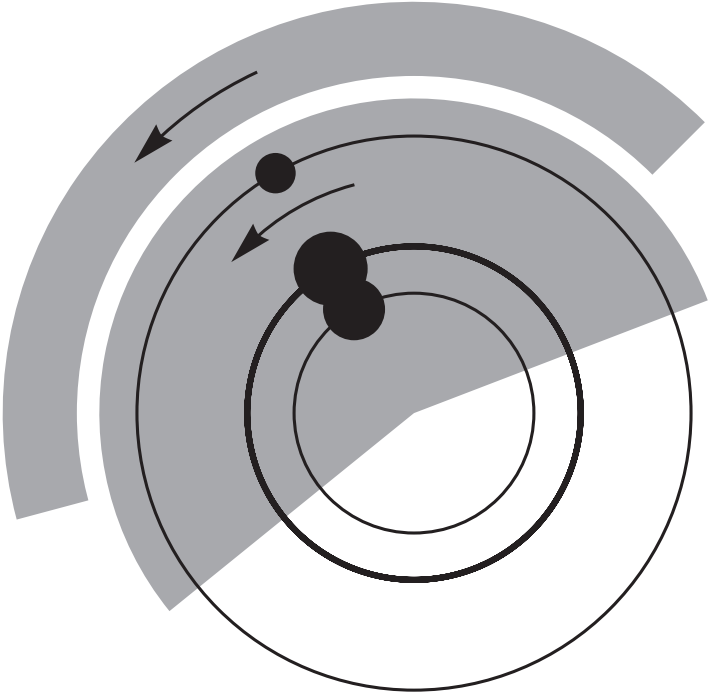

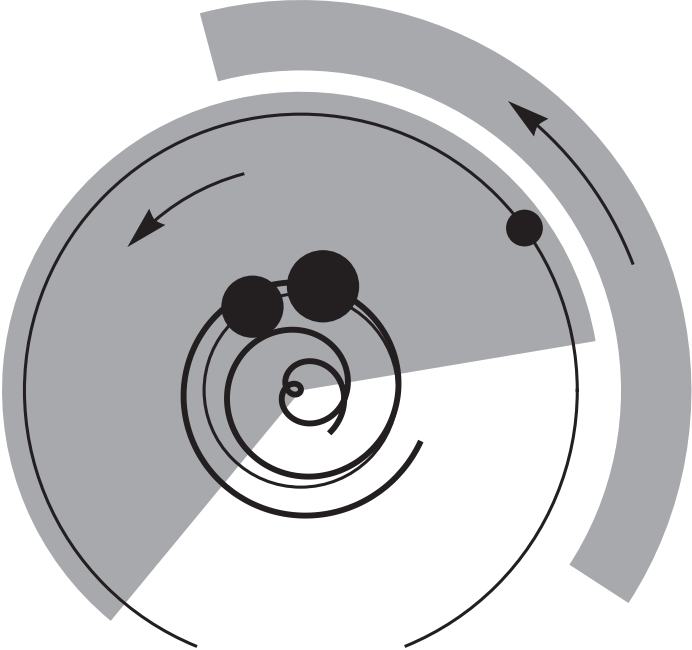

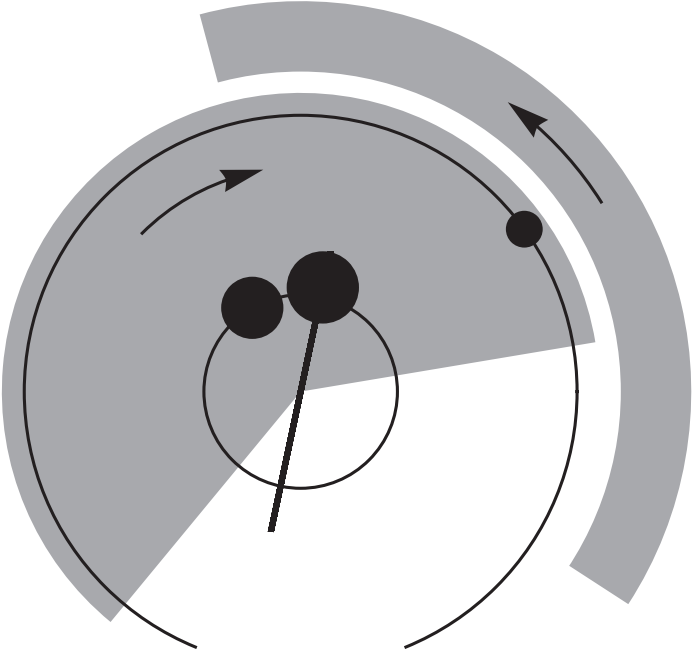

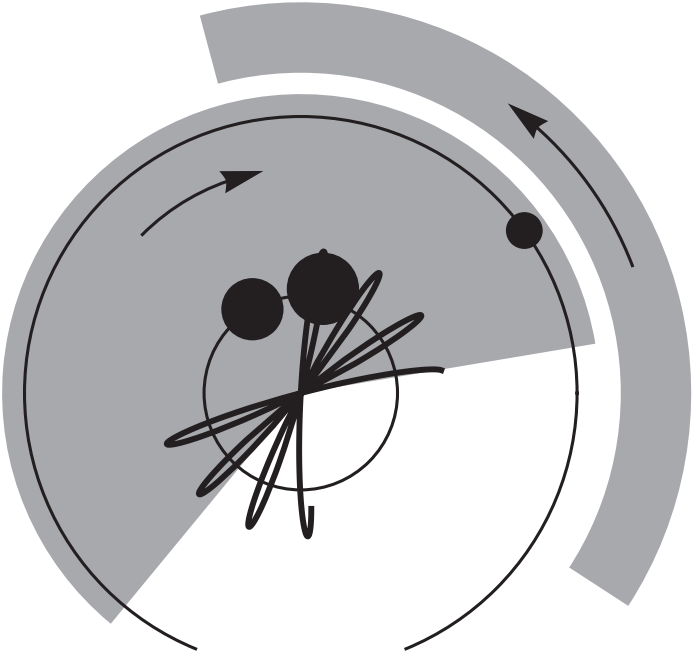

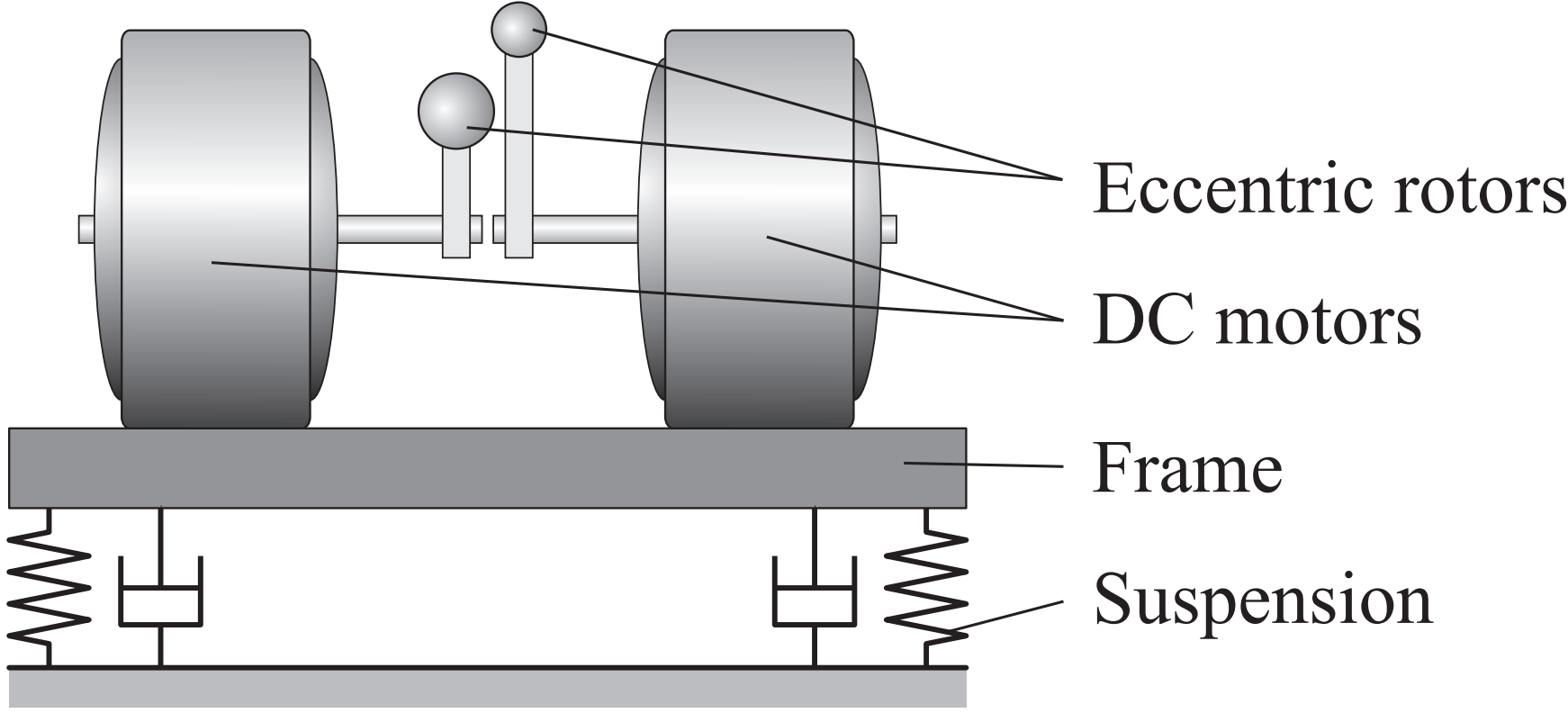
Eccentric rotors
DC motors
Frame
Suspension

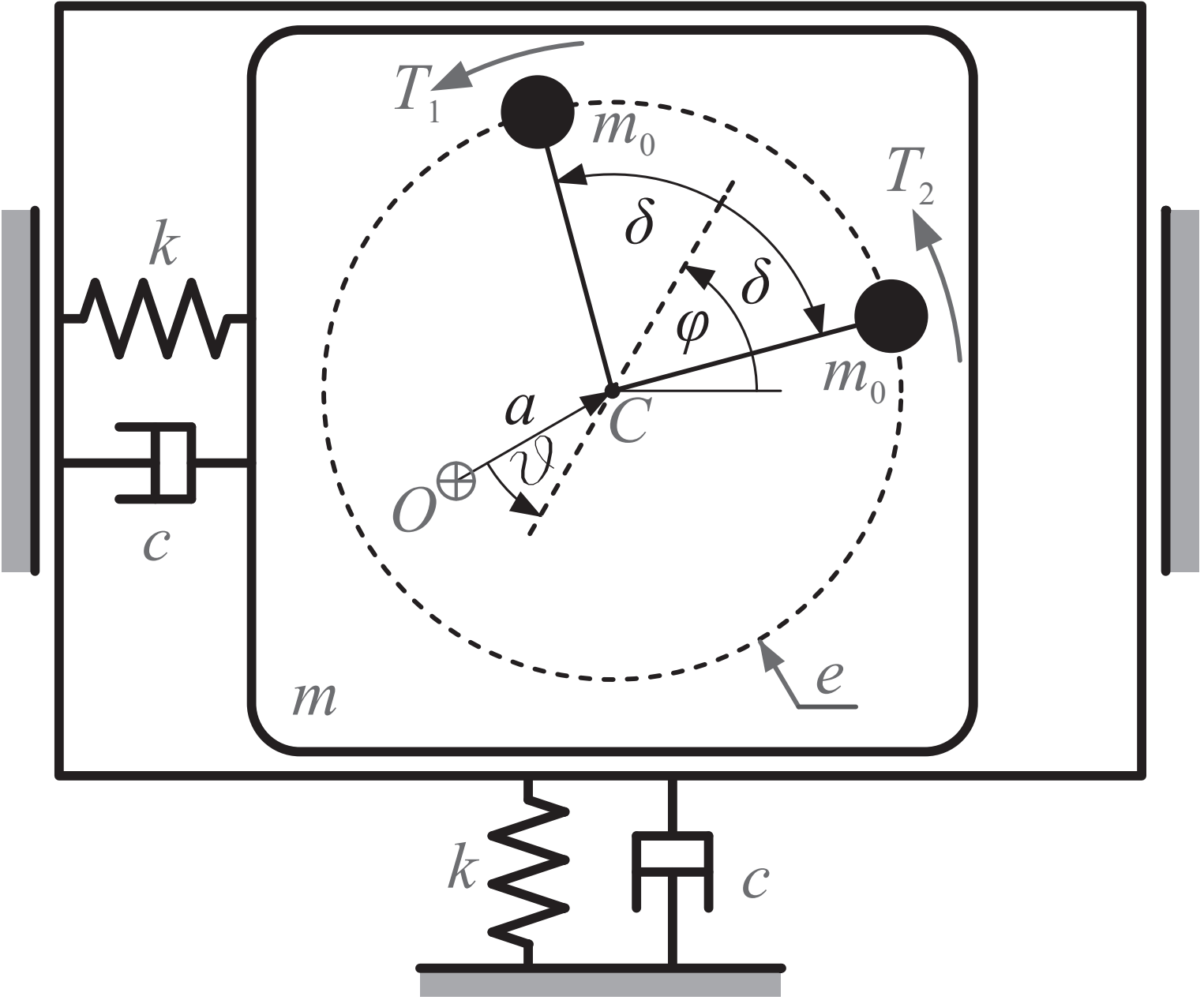
T_1
m_0
T_2
δ
δ
φ
m_0
k
a
C
ϑ
O
c
m
e
k
c

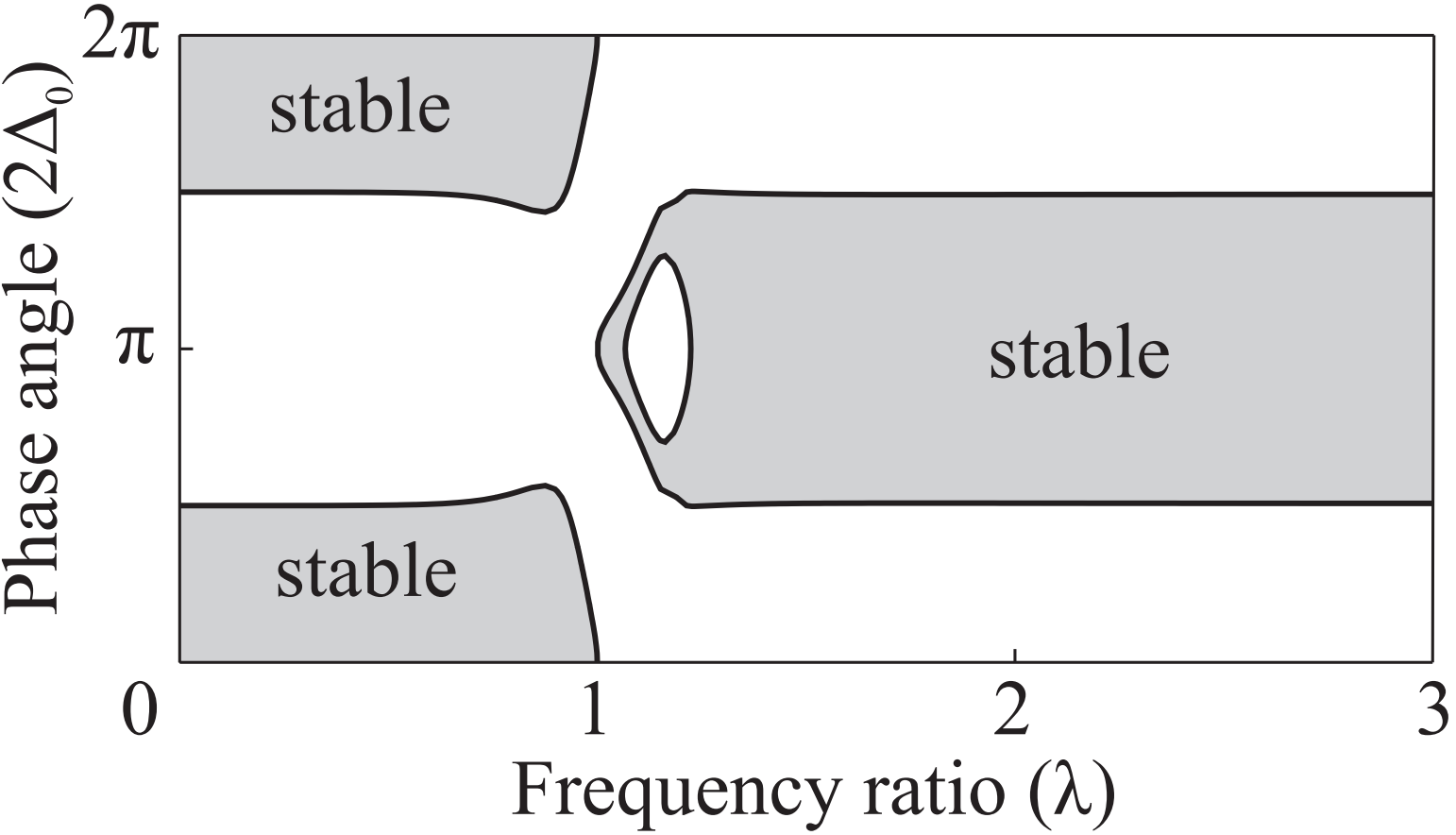
2π
π
0
stable
stable
stable
Phase angle (2Δ0)
1
2
3
Frequency ratio (λ)

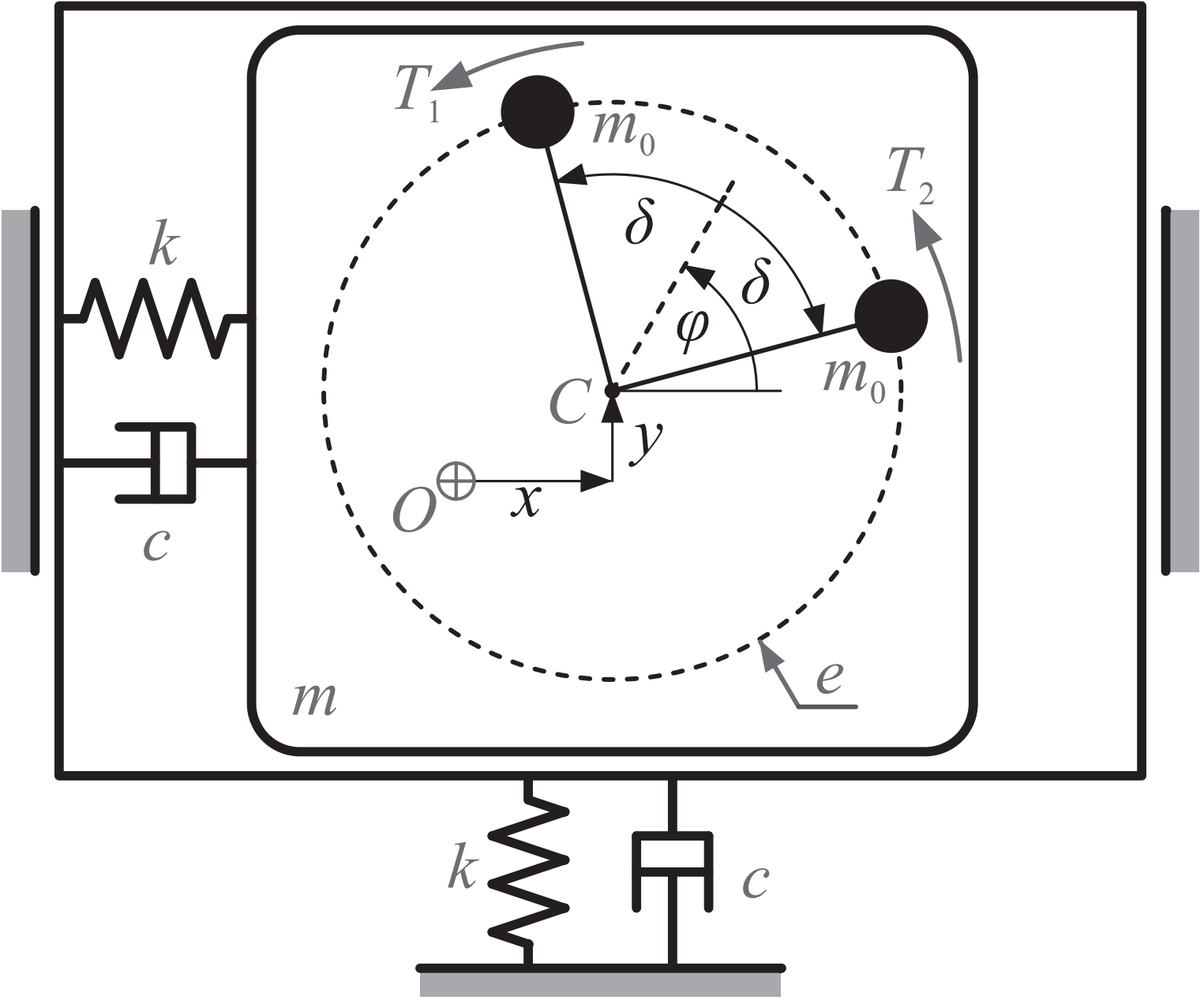
T_1
m_0
T_2
δ
δ
φ
m_0
k
C
y
c
O
x
m
e
k
c

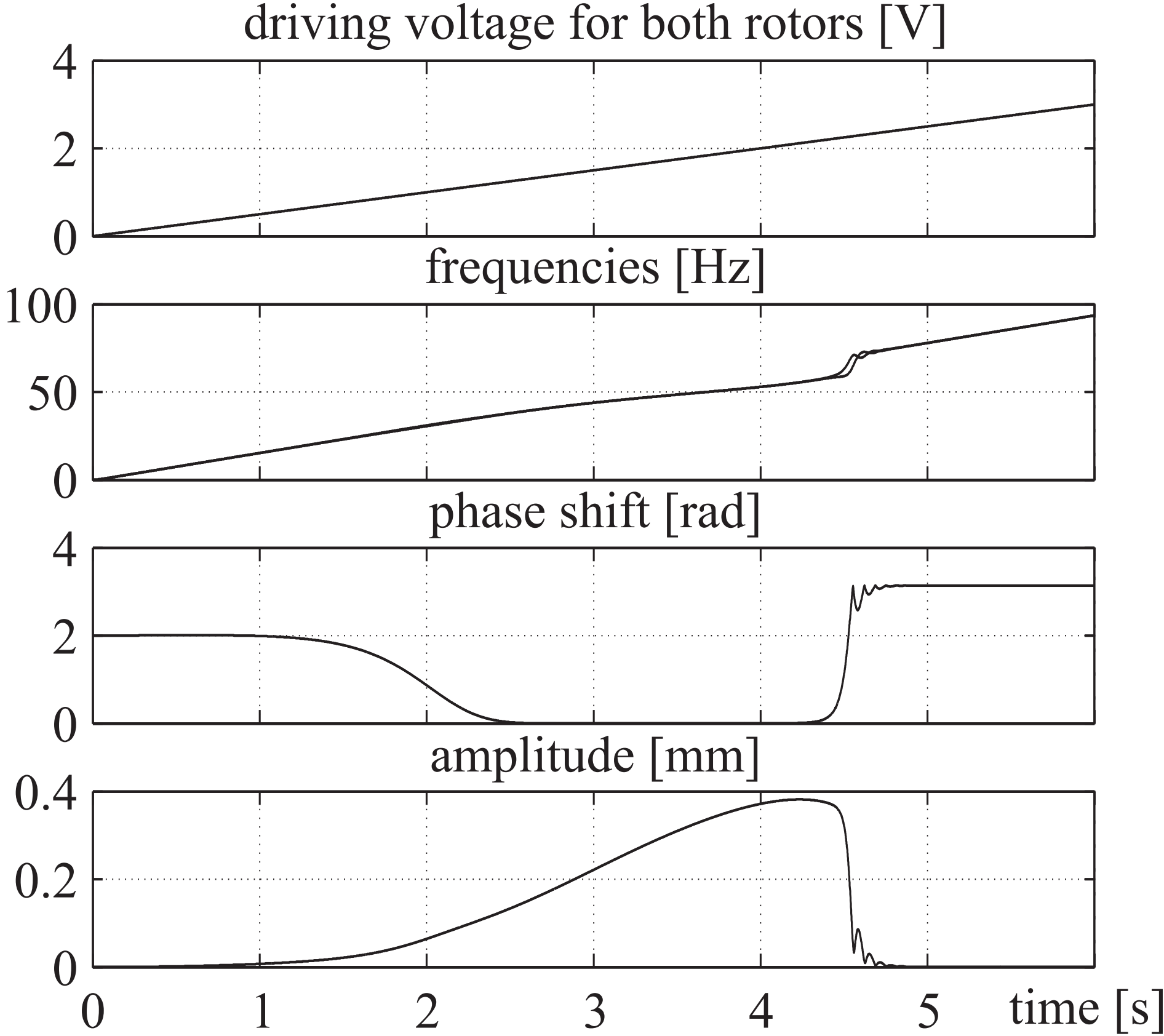
driving voltage for both rotors [V]
4
2
0
frequencies [Hz]
100
50
0
phase shift [rad]
4
2
0
amplitude [mm]
0.4
0.2
0
0
1
2
3
4
5
time [s]

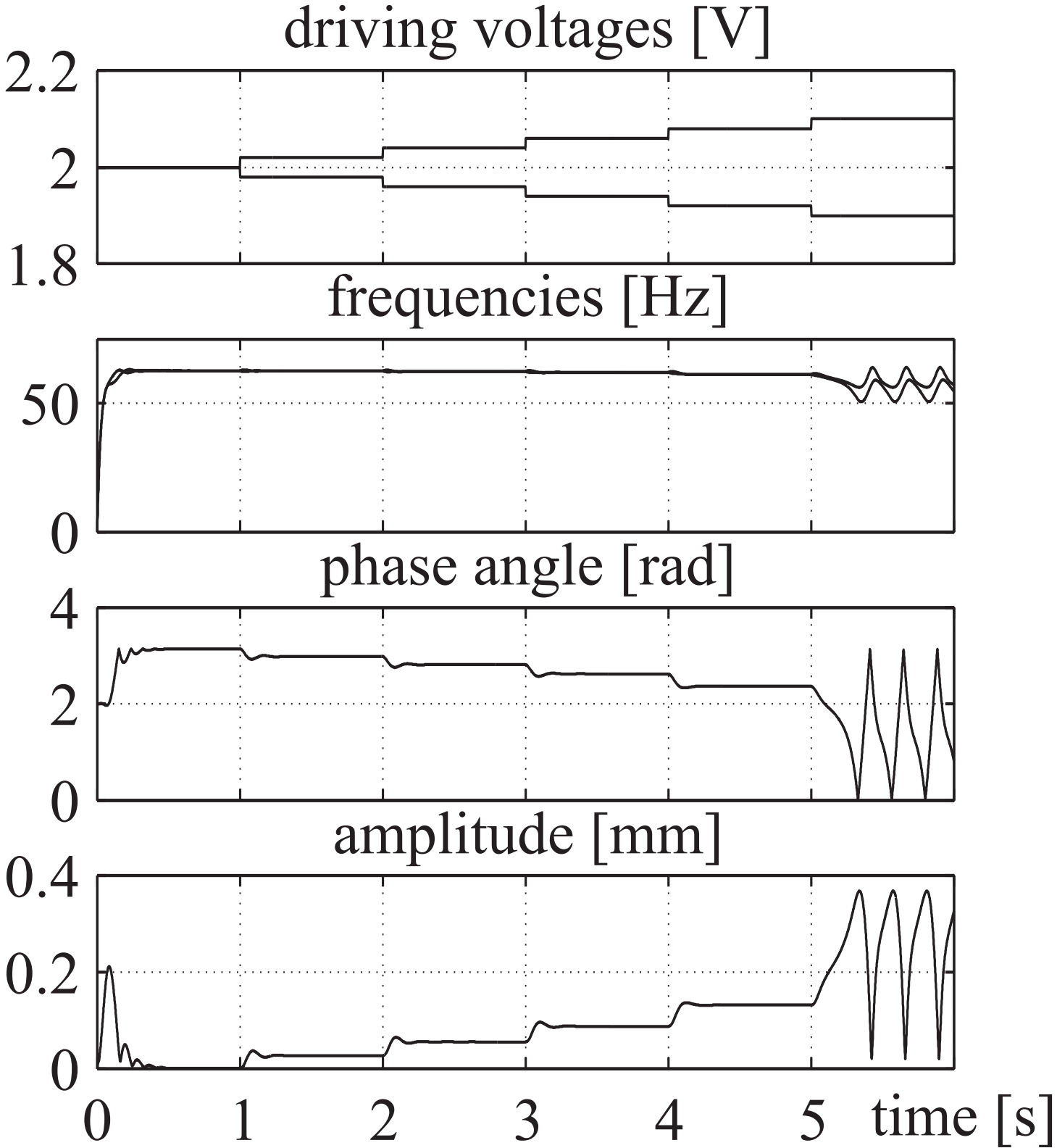
driving voltages [V]
2.2
2
1.8
frequencies [Hz]
50
0
phase angle [rad]
4
2
0
amplitude [mm]
0.4
0.2
0
0
1
2
3
4
5
time [s]

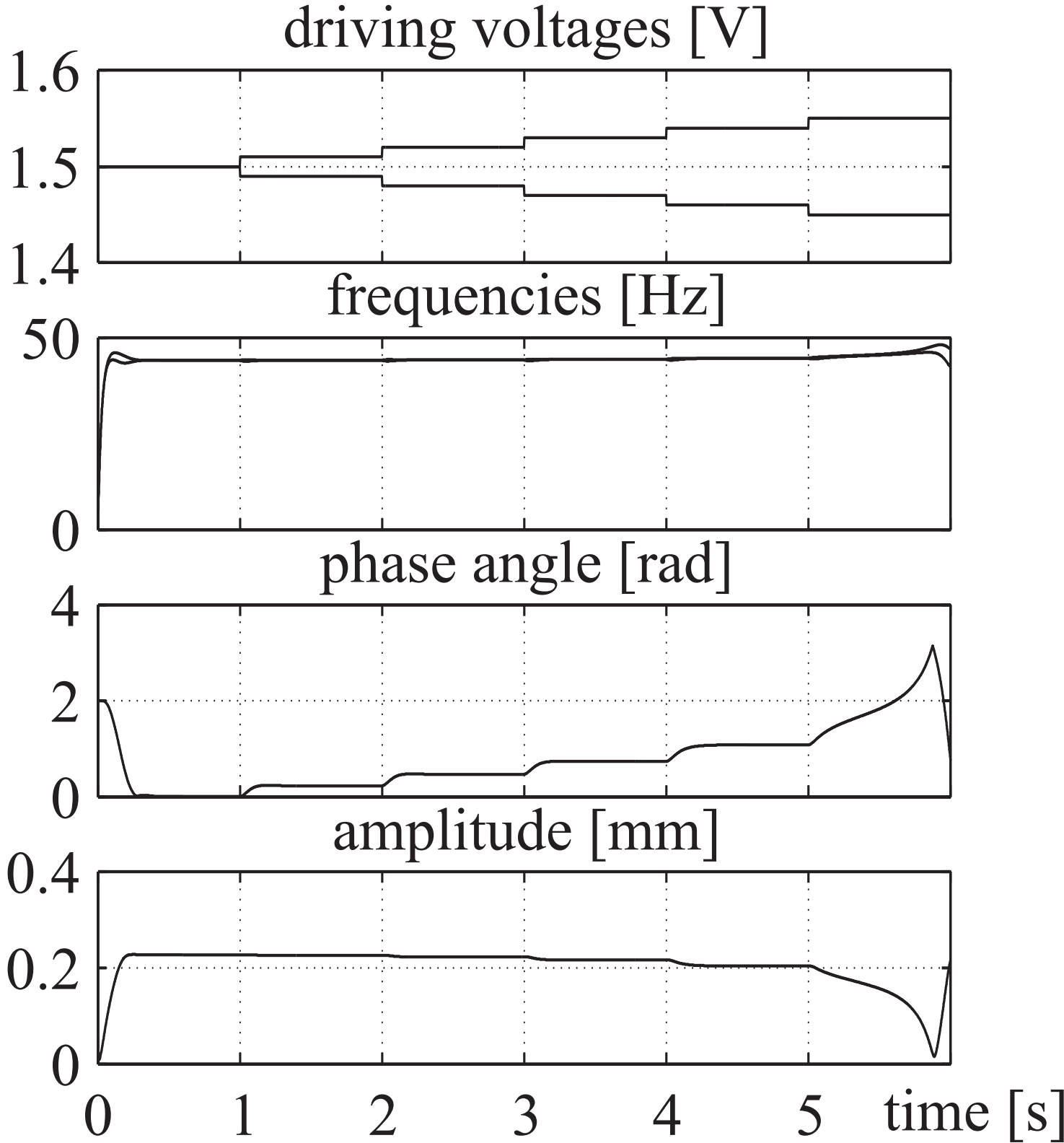
driving voltages [V]
1.6
1.5
1.4
frequencies [Hz]
50
0
phase angle [rad]
4
2
0
amplitude [mm]
0.4
0.2
0
0
1
2
3
4
5
time [s]

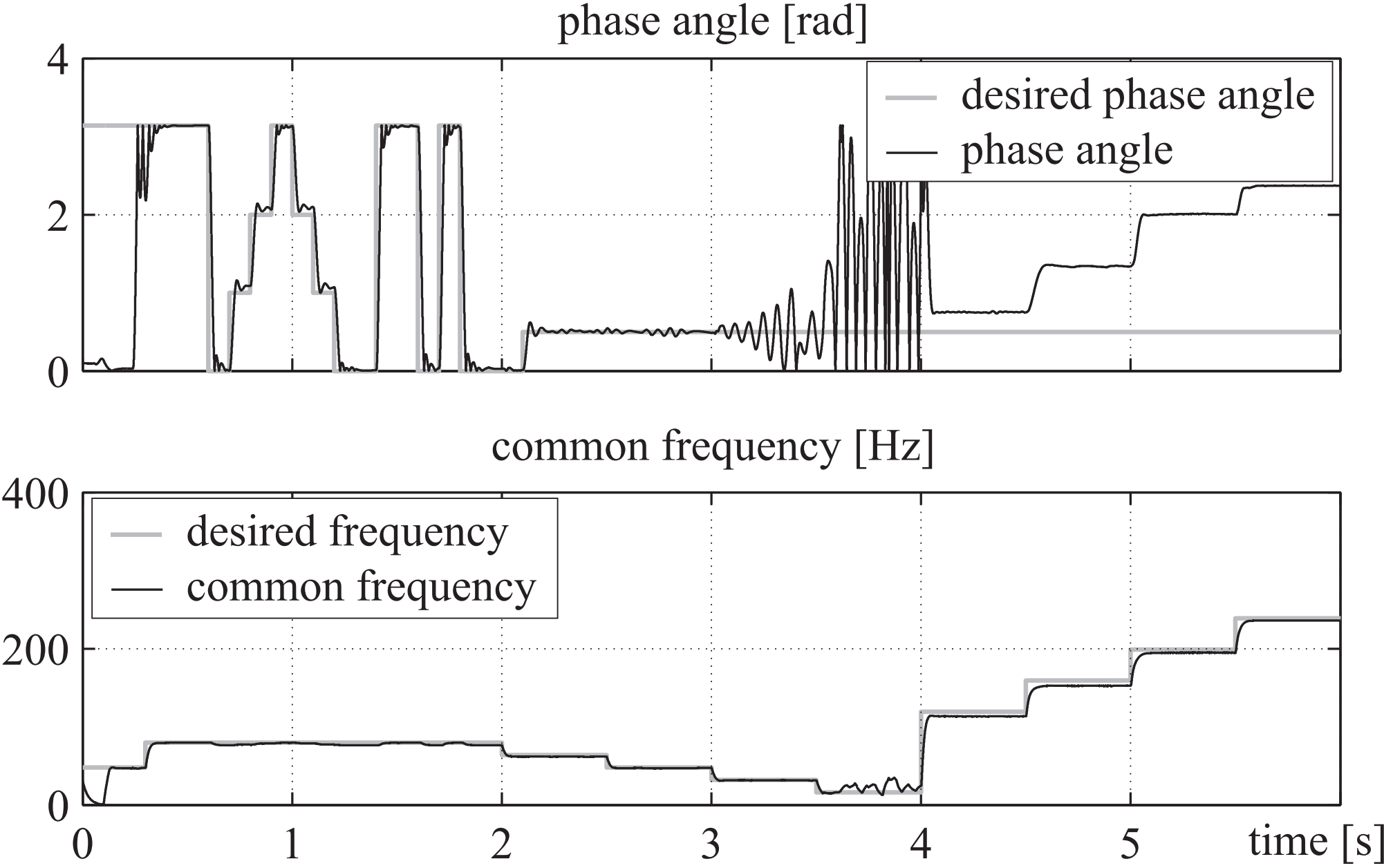
phase angle [rad]
4
2
0
desired phase angle
phase angle
common frequency [Hz]
400
200
0
desired frequency
common frequency
0
1
2
3
4
5
time [s]

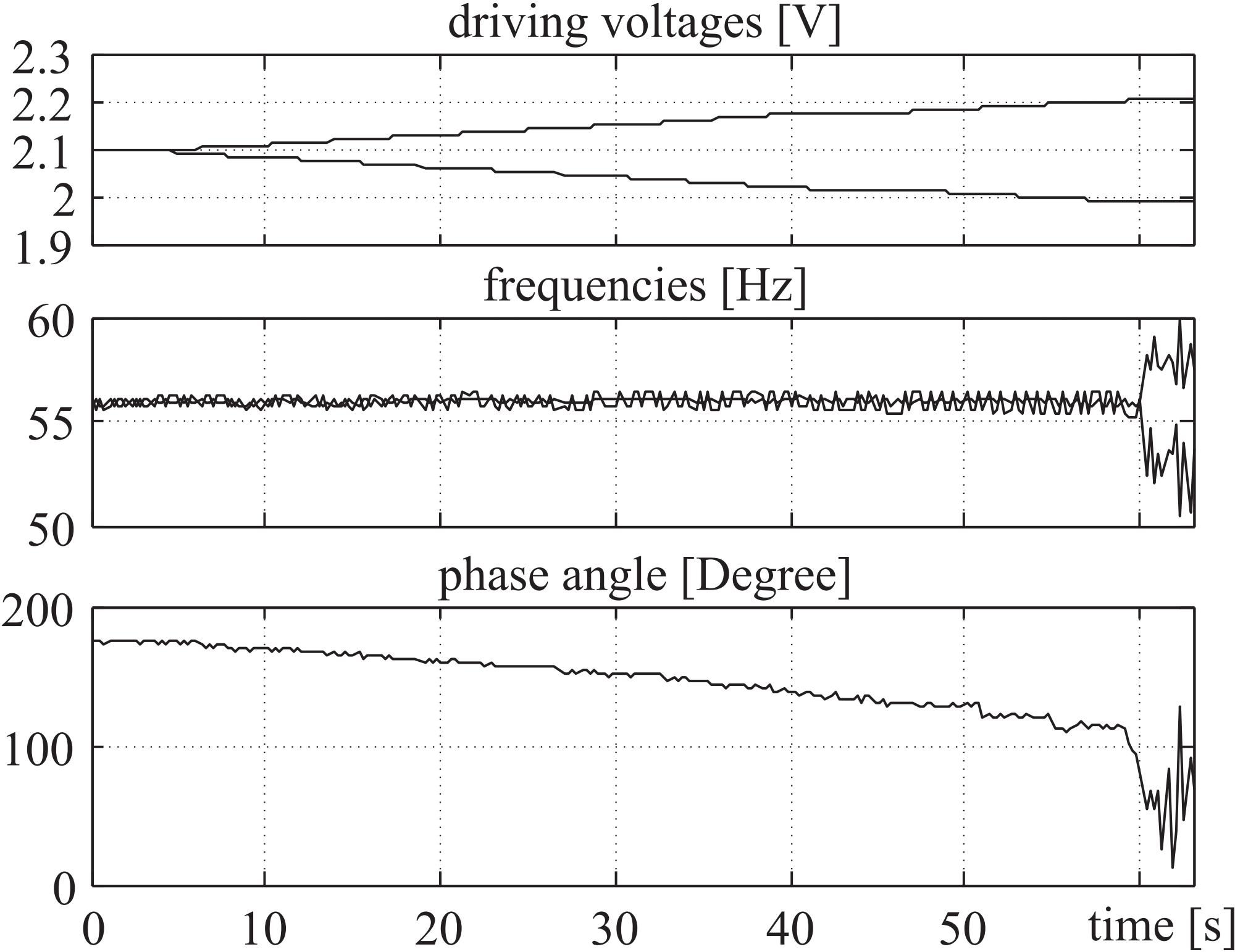
driving voltages [V]
2.3
2.2
2.1
2
1.9
frequencies [Hz]
60
55
50
phase angle [Degree]
200
100
0
0
10
20
30
40
50
time [s]

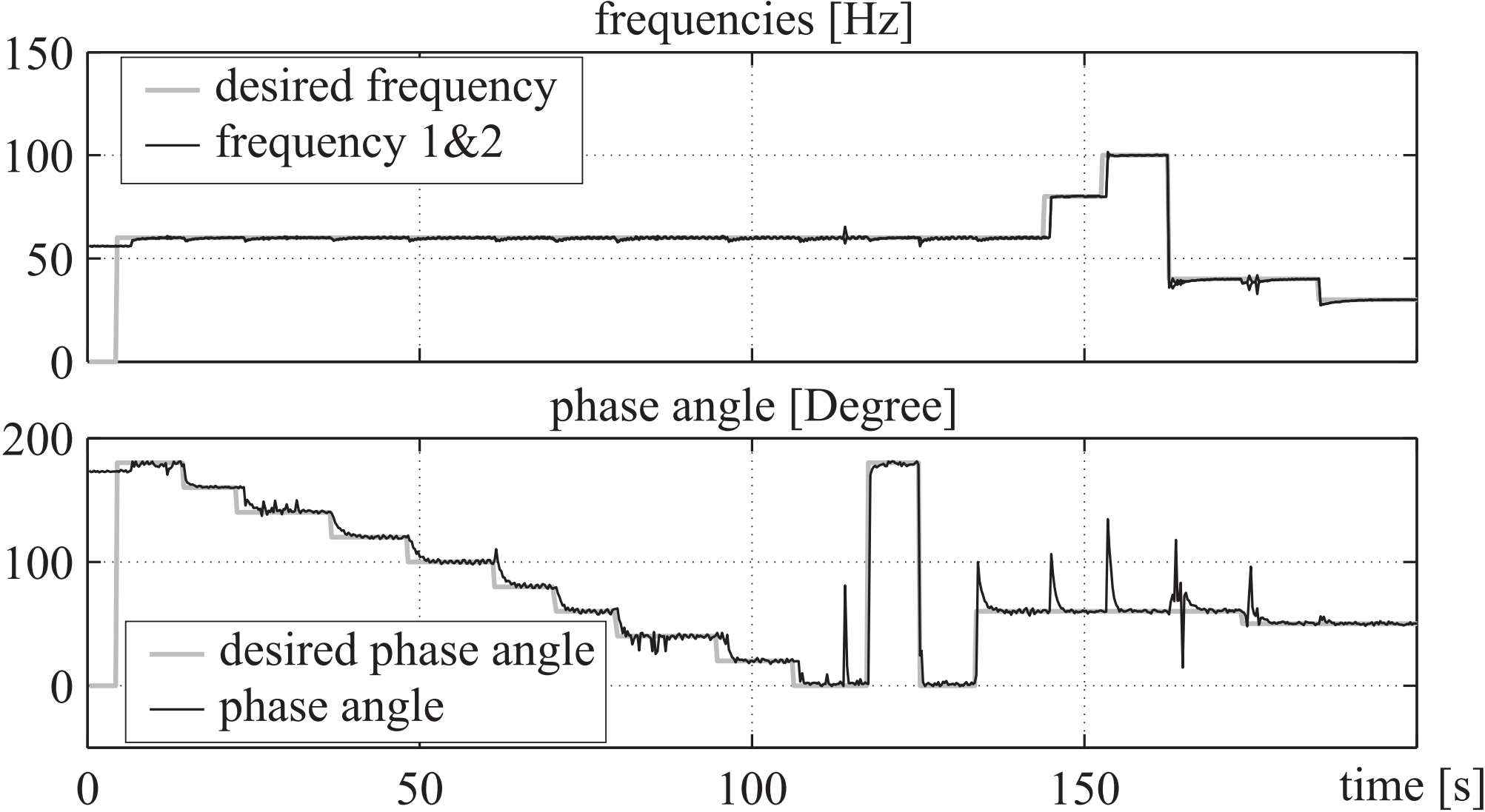
frequencies [Hz]
150
100
50
0
desired frequency
frequency 1&2
phase angle [Degree]
200
100
0
desired phase angle
phase angle
0
50
100
150
time [s]